

## Article

# pH-Responsive Eco-Friendly Chitosan–Chlorella Hydrogel Beads for Water Retention and Controlled Release of Humic Acid

Hao Li <sup>1,2</sup> , Jin Wang <sup>1,2</sup>, Yu Luo <sup>1,2,\*</sup>, Bo Bai <sup>1,2,\*</sup> and Fangli Cao <sup>3</sup>

<sup>1</sup> Key Laboratory of Subsurface Hydrology and Ecological Effect in Aird Region of the Ministry of Education, Chang'an University, Xi'an 710054, China; lh980726@163.com (H.L.); w15129938277@163.com (J.W.)

<sup>2</sup> School of Water and Environment, Chang'an University, Xi'an 710054, China

<sup>3</sup> SCEGC Installation Group Company Ltd., Xi'an 710054, China; 13772425276@163.com

\* Correspondence: 13289367808@163.com (Y.L.); baibochina@163.com (B.B.)

**Abstract:** For improving the mechanical strength of controlled release fertilizer (CRF) hydrogels, a novel material of *Chlorella* was employed as a bio-based filler to prepare chitosan–chlorella hydrogel beads with physical crosslink method. Here, the synthesis mechanism was investigated, and the chitosan–chlorella hydrogel beads exhibited enhanced mechanical stability under centrifugation and sonication than pure chitosan hydrogel beads. *Chlorella* brought more abundant functional groups to original chitosan hydrogel, hence, chitosan–chlorella hydrogel beads represented greater sensitivity and controllable response to external factors including pH, salt solution, temperature. In distilled water, the hydrogel beads with 40 wt% *Chlorella* reached the largest water absorption ratio of 42.92 g/g. Moreover, the mechanism and kinetics process of swelling behavior of the chitosan–chlorella hydrogel beads were evaluated, and the loading and releasing of humic acid by the hydrogel beads as a carrier material were pH-dependent and adjustable, which exhibit the potential of chitosan–chlorella hydrogel beads in the field of controlled release carrier biomaterials.



**Citation:** Li, H.; Wang, J.; Luo, Y.; Bai, B.; Cao, F. pH-Responsive Eco-Friendly Chitosan–Chlorella Hydrogel Beads for Water Retention and Controlled Release of Humic Acid. *Water* **2022**, *14*, 1190. <https://doi.org/10.3390/w14081190>

Academic Editor: Adriana Bruggeman

Received: 27 February 2022

Accepted: 5 April 2022

Published: 8 April 2022

**Publisher's Note:** MDPI stays neutral with regard to jurisdictional claims in published maps and institutional affiliations.



**Copyright:** © 2022 by the authors. Licensee MDPI, Basel, Switzerland. This article is an open access article distributed under the terms and conditions of the Creative Commons Attribution (CC BY) license (<https://creativecommons.org/licenses/by/4.0/>).

**Keywords:** hydrogel; controlled release; swelling; *Chlorella*; pH sensitivity

## 1. Introduction

Fertilizer is an indispensable part of modern agriculture. The proper application of fertilizers can maintain soil fertility and improve crop yields. However, during the volatilization and leaching process, fertilizer losses have greatly reduced the utilization efficiency, increased agricultural costs and threatened environmental pollution, especially in developing countries [1]. Recently, controlled release fertilizers have received considerable attention worldwide with the potential to achieve a partial synchronization of nutrient release and physiological need of plants which can effectively prevent fertilizer losses [2]. Polymer, using as the initial material of hydrogel, has been proven to be an effective prolonged-release carrier for the advantage of absorbing a high amount of water and release it over a long period of time in combination with a fertilizer [3–5]. The combination of hydrogel and fertilizer, like a “mini reservoir”, reduces both the environmental impact of fertilizer and evaporation losses. However, a large amount of polymers such as poly(acrylic acid), poly(acrylamide), and copolymer are difficult to biodegrade [3]. Consequently, seeking biodegradable, abundant, and low-cost natural polymers for controlled release fertilizers have become a priority for engineers [6].

Chitosan, the product of deacetylation of the natural polysaccharide chitin, is a commonly used biomaterial composed of  $\beta$ -(1-4)-2-acetamido-D-glucose and  $\beta$ -(1-4)-2-amino-D-glucose units, with a  $pK_a$  value varying from 6.3 to 6.5 [7,8]. Chitin, mainly derived from crustaceans such as shrimp and crab, is one of the most plentiful biopolymers on Earth [9], and hence crab and shrimp shell waste provides a sufficient source for the industrial production of chitosan. There are three types of reactive functional groups in chitosan, an

amino/acetamido group as well as both primary and secondary hydroxyl groups at the C-2, C-3, and C-6 positions, respectively [7]. The amino group is responsible for differences in structure and physico-chemical properties due to its intra/inter-molecular hydrogen bonds. The chemical and physical properties of chitosan depend on the molecular weight (MW), degree of deacetylation (DDA), and degree of crystallinity, extent of ionization/free amino group [7]. The physico-chemical properties, which include viscosity, solubility, adsorption on solids, elasticity, tear strength, and bio-functional activities, are dependent on the molecular weight of the polymer concerned [7]. The molecular weight of chitosan also affects the crystal size and morphological character [10]. The drug release from chitosan hydrogels is related to the molecular weight of chitosan. Generally, as the molecular weight of chitosan increases, the rate of drug release into the biological medium decreases [11]. With exceptional biocompatibility and biodegradability, chitosan has proven to be an effective prolonged-release carrier. For example, Wu and colleagues prepared colon-targeted chitosan/alginate hydrogel beads by using chitosan and sodium alginate as cross-linking agents and used hydrogel beads for a colon-targeted release of doxorubicin hydrochloride (DOX) [12]. However, the limited chain flexibility and poor mechanical strength of chitosan hydrogels have imposed difficulties on the wide application of chitosan. Generally, cross-linking techniques with crosslinkers and inorganic fillers are effective methods to improve the mechanical strength of chitosan-based hydrogels [13]. Shawkyy prepared a variety of composite microspheres of chitosan with carbon nanotubes as fillers to improve the removal of mercury (II) from water by chitosan [14]. Some studies have also combined montmorillonite with chitosan to enhance the adsorption capacity of the material [15]. However, these introduced substances were difficult to degrade and are not environmentally friendly. Bio-based fillers have the advantages of abundant sources, low cost, and biodegradability, and their use will not create new environmental problems [16]. Bio-fillers obtained from agricultural waste such as sugarcane bagasse, soy protein, wheat straw, and rice husk are also used to reinforce polymers because of their abundance and as an economical solution for waste management [16]. In addition, the physical properties of the bio-based filler, such as hydrophobicity, are also factors to be considered. If the filler and the matrix are not compatible, modification of the filler needs to be considered [17]. Therefore, in order to improve the performance of chitosan hydrogels, it is essential to select bio-based fillers which are biodegradable, compatible with chitosan, and provide excellent mechanical performance.

*Chlorella* is a spherical, unicellular microalga with a diameter of 3–8  $\mu\text{m}$ . It grows by photosynthesis and can be found in both freshwater and seawater, with many species [18]. *Chlorella* is one of the most widely cultured microalgae species because it is nutrient-rich, ideal for production, fast-growing, and requires only sunlight and nutrients to grow and reproduce in a short period of time, which provides a wide and inexpensive source of *Chlorella* [19]. Structurally, *Chlorella* is comprised of the cell wall, cell membrane, cytoplasm, chloroplast, nucleus, vacuoles, and mitochondria [20]. It has a remarkably robust cell wall, mainly composed of cellulose, hemicellulose, proteins, and lipids [20], which have ample functional groups such as hydroxyl (-OH), carboxyl (-COOH), amino (-NH<sub>2</sub>), and amide groups (-CONH<sub>2</sub>) [21]. These hydrophilic functional groups would form a large number of hydrogen bonds with chitosan, resulting in stronger van der Waals and electrostatic effects, making the chemical bonding interactions between *Chlorella* cells and chitosan stronger than inorganic fillers. Moreover, the tough cell wall of *Chlorella* has excellent tensile strength, which can provide the required mechanical performance for chitosan hydrogels [22]. In addition, the cell wall of *Chlorella* not only protects cells from external invasion but also has semi-permeable property, that is, each cell presents as a hollow structure that allows water molecules to permeate through. The space inside the *Chlorella* cells may act like a miniature reservoir to accumulate water, thereby improving the water retention properties of chitosan hydrogel beads [23]. On the other hand, natural fibers which are often used as bio-based fillers, such as cotton, jute, hemp, and flax require fertile land for cultivation [24]. Therefore, one of the advantages of *Chlorella* is that it does not compete with agricultural

crops for valuable arable land. To our knowledge, there are few studies using *Chlorella* as a bio-based filler to enhance the properties of natural polymers.

The awareness about the environment and sustainability has led to the demand for alternative petroleum-based polymer products, such as natural polymers reinforced with bio-based fillers. Inspired by these, *Chlorella* has been selected as a novel material to employ as a bio-based filler to reinforce polymer performance. In this paper, chitosan–chlorella hydrogel beads have been manufactured through the physical crosslinking method. Considering that the cellular structure and biochemical properties of *Chlorella* can strengthen the mechanical strength and water absorption properties of chitosan hydrogels, we investigate the relevant properties of the prepared chitosan–chlorella hydrogels. Similarly, the surface structure of the chitosan–chlorella hydrogel beads was investigated with scanning electron microscopy (SEM), and their structure was characterized with Fourier transform infrared spectroscopy (FTIR). Moreover, we discuss the swelling mechanism and kinetics to study the swelling process in water. Finally, in order to evaluate the feasibility of hydrogel beads for controlled release fertilizers, their pH and temperature stimuli-responsive release behavior for the slow release of humic acid was investigated.

## 2. Materials and Methods

### 2.1. Experimental Materials

Food-grade *Chlorella* powder was purchased from Shengqing Biotechnology Co., Ltd. (Xi'an, China). Chitosan (degree of deacetylation  $\geq 0.90$  and  $M_w = 700,000$ – $800,000$ ) was purchased from Sinopharm Chemical Reagent Co., Ltd. (Shanghai, China) Analytic-grade glacial acetic acid, sodium chloride (NaCl), potassium chloride (KCl), calcium chloride ( $\text{CaCl}_2$ ), magnesium chloride ( $\text{MgCl}_2$ ), aluminum chloride ( $\text{AlCl}_3$ ), sodium hydroxide (NaOH), hydrochloric acid (HCl), etc., were provided by Shanghai Aladdin Biochemical Technology Co., Ltd. (Shanghai, China) Humic acid with a purity of no less than 90% was purchased from Shanghai Yuanye biotech Co., Ltd. (Shanghai, China).

### 2.2. Synthesis of Chitosan–Chlorella Hydrogel Beads

A 1 g amount of chitosan was added to 50 mL 2% (*v/v*) acetic acid solution, stirring constantly to dissolve the chitosan. Then, a certain amount of *Chlorella* powder was added to the chitosan solution and stirred continuously for 1 h. The above blended solution was dropped into a 2 M NaOH solution using a syringe needle with a diameter of 0.6 mm. This results in the formation of alkaline hydrogel beads. The formed chitosan–chlorella beads were left in NaOH solution for another 3 h for gelation. The beads were separated from the NaOH solution with a metal sieve and washed repeatedly until the solution pH became neutral. Then, the resulting sample was dried at room temperature to obtain the chitosan–chlorella hydrogel beads.

### 2.3. Materials Characterization

The dried chitosan and chitosan–chlorella hydrogel beads were ground into powder. Then, 1 mg of the powder was blended with 100 mg of KBr in an agate mortar and pressed into flakes after grinding evenly. Afterwards, FTIR infrared spectra were measured at  $4000$ – $450\text{ cm}^{-1}$  wavenumber in a Nicolet FTIR spectrometer. Surface morphology, shape, and size of the chitosan–chlorella hydrogel beads were investigated by scanning electron microscope.

### 2.4. Degree of Swelling Measurements

A known weight of dry hydrogel sample was submerged in 250 mL swelling media (distilled water, various salt solutions, and buffer solutions with desired pH) and remained at room temperature for 4 h until the swelling equilibrium was reached. The sample was

removed and absorbed the excess water with filter paper and weighed. The degree of swelling was obtained by the following formula:

$$S_d = \frac{W_e - W_i}{W_i} \quad (1)$$

where  $W_e$  and  $W_i$  are the weights of the hydrogel beads' swelling equilibrium and initial weights, respectively. In other words, the degree of swelling is calculated according to the grams of water absorbed per gram of sample.

### 2.5. Determination of Mechanical Stability

The mechanical stability of chitosan–chlorella hydrogel beads was judged by the response of the samples to ultrasonic vibration and centrifugation at high speed. The dried samples were left in distilled water for 4 h to reach swelling equilibrium. Then, a certain mass of swelling hydrogel beads was centrifuged at 4000 rpm or ultrasonified at 40 kHz, respectively. The mass of samples retained was weighed at distinct time intervals ( $t$ ; min). The weight retention rate was obtained by the following formula:

$$\text{Weight retention (\%)} = \frac{W_a}{W_e} \times 100 \quad (2)$$

where  $W_e$  and  $W_a$  are the wet weights of hydrogel beads before and after centrifugation or ultrasonification, respectively.

### 2.6. Loading and Slow-Release Efficiency for Humic Acid

To study the potentiality of chitosan–chlorella hydrogel beads as controllable loading and release carriers, humic acid was selected as a model fertilizer. Humic acid was loaded into the hydrogel beads with 40 wt% *Chlorella* content, so as to explore its feasibility in the controllable loading and release system. The 0.5 g dried hydrogel beads were placed in 50 mL 30  $\mu\text{g/mL}$  humic acid with pH from 4 to 12 and then shaken in a constant temperature shaker at 120 rpm for 30 min at 30 °C. The humic-acid-loaded hydrogel beads were oven dried at 30 °C after filtration separation. The concentration of humic acid solution in the supernatant was calculated by absorbance at 259.6 nm wavelength with a 752 UV-vis spectrophotometer [25]. The loading efficiency of humic acid was calculated by the following equation:

$$\text{Loading efficiency (\%)} = \frac{C_0 - C_1}{C_0} \times 100 \quad (3)$$

where  $C_0$  and  $C_1$  are the concentrations at the initial and end of the loading of humic acid, respectively.

The humic-acid-loaded samples were immersed in distilled water with various pH and shaken in a constant temperature shaker at 120 rpm for 3 h. The concentration of humic acid in the mixed solution was determined at intervals, and the release efficiency of humic acid was calculated by the following equation:

$$\text{Release efficiency (\%)} = \frac{2C_2}{C_0 - C_1} \times 100 \quad (4)$$

where  $C_2$  is the concentration of humic acid after release.

## 3. Results and Discussion

### 3.1. Synthesis and Characterization of Chitosan–Chlorella Hydrogel Beads

The preparation mechanism of the chitosan–chlorella hydrogel beads is shown in Figure 1. Chitosan, with a  $pK_a$  value of about 6.3, can be dissolved in dilute acid, but not in water or alkaline medium because the amino group ( $-\text{NH}_2$ ) in the structural unit can be reacted with acid readily and converted into soluble protonated amino group ( $-\text{NH}_3^+$ ) [26].

Therefore, an acidic solution was often used as the solvent for dissolving chitosan. In this study, a 2% acetic acid solution was used to dissolve chitosan. After a long time stirring, chitosan powder was completely dissolved in acetic acid solution, during which the hydroxyl, amino, and N-acetylamino groups distributed on the chitosan macromolecule chain interact to form various intra- and intermolecular hydrogen bonds. As a result, the molecular chains of chitosan were intertwined under the action of hydrogen bonding and van der Waals forces, thus forming a three-dimensional network structure [27]. Meanwhile, the  $\text{-NH}_2$  group of glucosamine monomer on chitosan molecular chains were protonated into positively charged  $\text{-NH}_3^+$  groups in acidic environment, and electrostatic repulsion between  $\text{-NH}_3^+$  groups expanded the three-dimensional network. *Chlorella* powder was subsequently added into chitosan solution, the expansion caused by electrostatic repulsion made it easier for *Chlorella* cells to disperse and embed into the chitosan network uniformly. Then, the chitosan–*chlorella* mixture solution was dripped into sodium hydroxide solution through a needle. At alkaline conditions,  $\text{-NH}_3^+$  groups were deprotonated, and the solubility of chitosan was reduced and precipitated out of the solution, resulting in the formation of hydrogel beads. During the synthesis process, the changing process from high viscosity droplets to hydrogel beads can be clearly observed, and these changes in its shape and morphology confirmed the formation of hydrogel. Therefore, it can be concluded that the *Chlorella* cells were successfully encapsulated into the chitosan cross-linked network and the chitosan–*chlorella* hydrogel beads were synthesized.

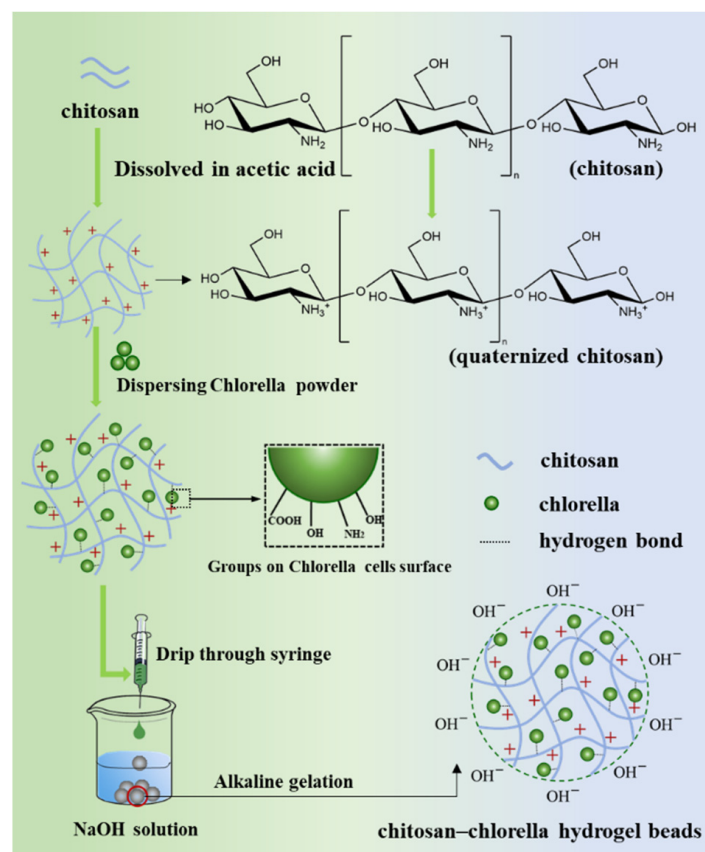


**Figure 1.** Mechanism of formation of chitosan–*chlorella* hydrogel beads.

The FTIR spectra of *chlorella*, chitosan beads, and chitosan–*chlorella* hydrogel beads are shown in Figure 2. For chitosan, the peaks at  $1659$  and  $1326\text{ cm}^{-1}$  are attributed to the  $\text{-NH}_2$  deformation vibration and C–N stretching vibration, respectively [28]. The characteristic absorption band at  $3362$ ,  $1598$ , and  $1095\text{ cm}^{-1}$  are attributed to O–H hydroxyl group, N–H angular deformation, and C–O–C in glycosidic linkage, respectively [29]. For *Chlorella*, the broad peak at  $3301\text{ cm}^{-1}$  is due to the stretching vibration of intermolecular

hydroxyl, and the peak at  $1079\text{ cm}^{-1}$  is attributed to the C-O stretching vibration, which indicate the presence of abundant hydroxyl groups on *Chlorella* [30]. Furthermore, the characteristic absorption band at 1658, 1546, 1401, and  $1241\text{ cm}^{-1}$  are from C=O stretching vibration (amide I), N-H bending vibration (amide II), and C-N absorption band (amide III) in the amide, respectively [31]. In the FTIR spectra of chitosan–chlorella hydrogel beads shown in curves c and d, hydrogel beads with 20 wt% and 40 wt% *Chlorella* retained most of the characteristic peaks of chitosan and *Chlorella*. However, the absorption peaks of chitosan at 3362, 1095  $\text{cm}^{-1}$  and *Chlorella* at 3301, 1079  $\text{cm}^{-1}$  shifted in different degrees. Meanwhile, the absorption peaks of chitosan at 1659 and  $1326\text{ cm}^{-1}$  were also shifted. The shift in the characteristic peaks indicated that in the three-dimensional network of hydrogel beads, chitosan and *Chlorella* cells were connected and entangled together mainly through intermolecular hydrogen bonds between amino and hydroxyl groups, which result in a stable three-dimensional network.

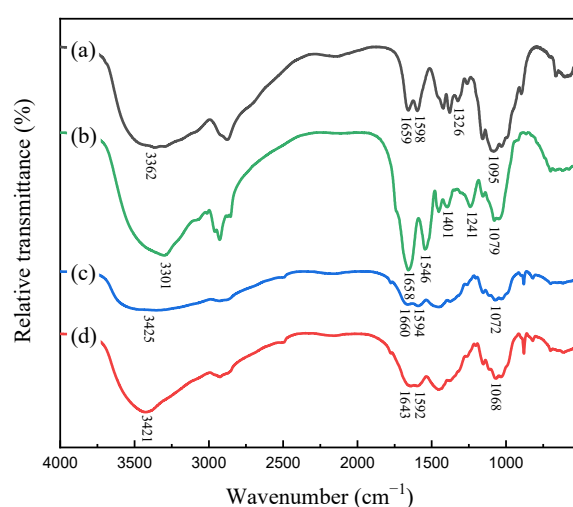


**Figure 2.** FTIR spectra of (a) chitosan, (b) *Chlorella*, (c) 20 wt% chitosan–chlorella hydrogel beads, and (d) 40 wt% chitosan–chlorella hydrogel beads.

Figure 3 provides the particle size image and SEM micrographs, which deliver the information on the size, shape, and surface topography of the hydrogel beads. It can be seen from Figure 3a that the diameter of swollen chitosan–chlorella hydrogel beads had an average size of 3 mm, while the average diameter of dried beads is about 0.9 mm. The increase of particle size indicated that the beads have a certain swelling ability. It can be seen that *Chlorella* cells are clustered with a diameter of 3–4 microns in Figure 3b. The chitosan–chlorella hydrogel beads shown in Figure 3d had a rougher surface and exhibited more severe shrinkage resulting from drying compared to the chitosan hydrogel beads with more perfect spherical shape in Figure 3c. However, the shrunken beads could still recover to full spherical shape after swelling, which was attributed to the three-dimensional network of hydrogel and stability of *Chlorella* cells. Figure 3e,f were the surface microtopography images of chitosan hydrogel beads and chitosan–chlorella hydrogel beads, respectively. Chitosan–chlorella hydrogel beads had more pores on the surface, with the average diameter of these pores being about  $0.2\text{ }\mu\text{m}$ . This porous structure brought about excellent adsorption properties to the hydrogel beads. In conclusion, landfilling of *Chlorella* cells enhanced the performance of hydrogel beads and exerted the advantages of composite materials.

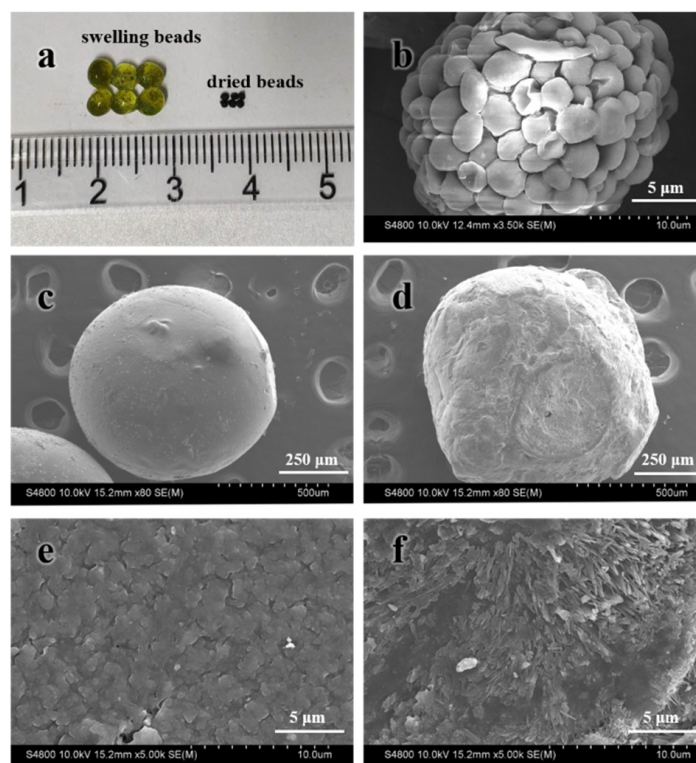


**Figure 3.** (a) Particle size image of chitosan–chlorella hydrogel beads swelling equilibrium and dried; (b) Clusters of *Chlorella* cells; (c) SEM micrographs of chitosan hydrogel beads; (d) SEM micrographs of chitosan–chlorella hydrogel beads; (e) surface microstructure of the chitosan hydrogel beads; (f) surface microstructure of the chitosan–chlorella hydrogel beads.

### 3.2. Mechanical Stability of Chitosan–Chlorella Hydrogel Beads

The mechanical stability of the chitosan–chlorella hydrogel beads was measured by the wet weight retention under ultrasound and centrifugation. Figure 4a shows the water retention of samples with different *Chlorella* content after a certain time of centrifugation. The van der Waals forces and hydrogen bonding, which are widely present between hydrogels and water molecules, determined the water retention properties of hydrogels [32]. In the first 20 min, the water retention rate decreased sharply, and then gradually slowed down. The reason for this phenomenon was that, the hydrogel beads contained more weakly bound water that was easier lost, and with the increase of centrifugal or ultrasonic time, the proportion of bound water that is difficult to separate became higher, resulting in a slower dehydration rate. After centrifugation for 60 min, the weight retention of chitosan hydrogel beads containing *Chlorella* was higher than that without *Chlorella*, and the higher the content of *Chlorella* in the beads, the higher the weight retention of beads. In other words, the presence of *Chlorella* enhanced the mechanical stability of hydrogel beads. The cross-linking of *Chlorella* with the chitosan network has strong hydrogen bonding interactions, the hydrogen bonds served as a crack bridge to retain an intact structure and stabilize the deformations of centrifugation. For example, Cong et al. have concluded that the intertwined hydrogen-bonding network of hydrogel could effectively relax the locally applied stress and dissipate the crack energy to improve the mechanical strength of hydrogel beads [33]. On the other hand, the natural toughness of the cell wall of *Chlorella* is resistant to the compressive forces brought about by centrifugation, preventing the hydrogel beads from being severely compressed.

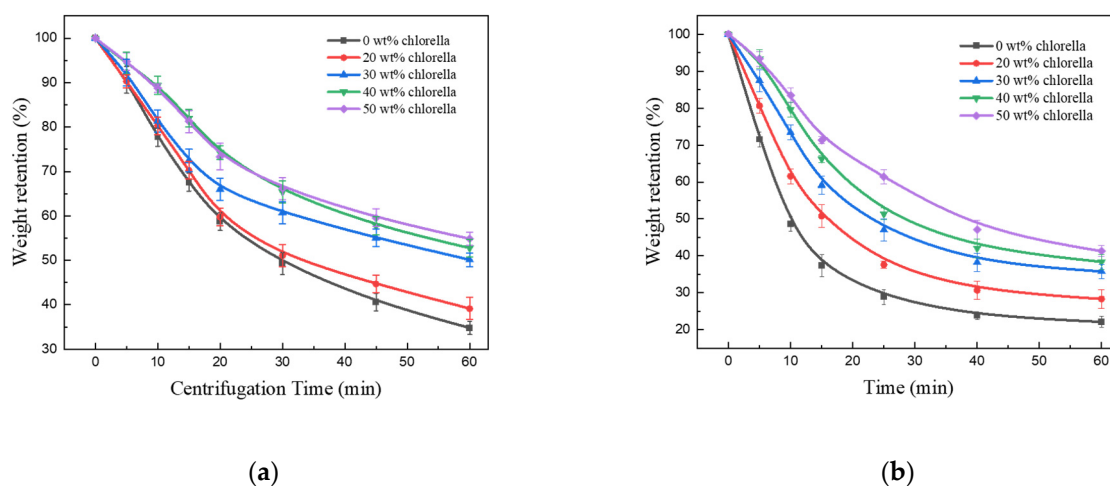


**Figure 4.** Weight retention of chitosan–chlorella hydrogel beads centrifuged at 4000 rpm (a) and ultrasonicated at 40 kHz (b).

Similar results were obtained from the ultrasonic experiments of chitosan–chlorella hydrogel beads as shown in Figure 4b. After ultrasonication for 60 min, water retention of the samples with higher *Chlorella* content was significantly higher than those with lower *Chlorella* contents. This indicated that the hydrogel beads formed by *Chlorella* with chitosan were more stable than the pure chitosan hydrogel beads in mechanical properties. The hydrophilic functional groups on the surface of *Chlorella* cells were linked together by strong hydrogen bonding interactions with -OH and -NH<sub>2</sub> groups on chitosan; thereby, the crosslinking of *Chlorella* cells and chitosan network increased the density of the crosslinked network and improved the physical strength of chitosan–chlorella hydrogel beads. In other words, the presence of abundant hydrogen bonds reinforced the skeletal structure of the chitosan hydrogel network. Therefore, the hydrogen bond cross-linked network formed by chitosan with *Chlorella* could better withstand ultrasonic fragmentation and keep the stability of beads. In summary, filling *Chlorella* into the hydrogel network with the effect of intermolecular forces can effectively reduce the water loss and improve the mechanical stability.

### 3.3. Swelling Behavior of Chitosan–Chlorella Hydrogel Beads

#### 3.3.1. Equilibrium Swelling Ratio at Various pH Solutions and Pulsatile Behavior

It is well known that the swelling behavior of hydrogels is significantly related to the pH of the swelling medium [34,35]. Therefore, the variety of the swelling ratio of chitosan–chlorella hydrogel beads based on pH change was investigated, and the swelling medium was buffer solutions with pH ranging from 2 to 10 at room temperature. In this study, the influence of ionic strength during the swelling process was avoided by using HAc–NaAc buffer solution, and the pH was controlled only by the dropwise addition of HCl or NaOH solution.

Figure 5a demonstrates the swelling behavior of hydrogel beads with different contents of *Chlorella* in the buffer solution of pH from 2 to 10. The chitosan–chlorella hydrogel beads reached maximum swelling at pH 6–8, and the order of the swelling ratios for samples with different *Chlorella* content was: 40 wt% > 30 wt% > 50 wt% > 20 wt% > 0 wt%. When the *Chlorella* content was lower than 40 wt%, the swelling degree increased with the increase in the *Chlorella* content. This is because the *Chlorella* cell may serve as a site for the storage of water in the cross-linked network, and the water molecules enter the intracellular of *Chlorella* after entering the cross-linked network by osmosis. This suggests that the presence of *Chlorella* enhanced the swelling capacity of the hydrogel beads. When the pH is lower than 6, the swelling degree increases with the increase in the pH value. However, when the pH exceeds 8, the swelling degree started to go down. The reason for this result was that when the pH value of the external solution was lower than the  $pK_a$  (approximately 6.3) of

chitosan, chitosan's amino groups were protonated, thus electrostatic attraction between  $-\text{NH}_3^+$  dilates the cross-linked network of the chitosan–chlorella hydrogel, which leads to an enhancement in swelling. However, the hydrogen bond formed by  $-\text{OH}$  on chitosan hindered the expansion of the network. In addition, chitosan can be dissolved in acidic solution. The corrosion of the chitosan–chlorella hydrogel beads by the external solution destroys the crosslinking network structure and leads to the decrease of swelling degree. Conversely, at high pH (above about 8), the  $-\text{NH}_3^+$  on chitosan was deprotonated to amino group, the influence of electrostatic attraction on crosslinking network is weakened. Besides, the hydrogen bonding induced by  $-\text{OH}$  and  $-\text{NH}_2$  and the “screening effect” of excess  $\text{Na}^+$  in external solution are also the reasons for the decrease of swelling degree [36].

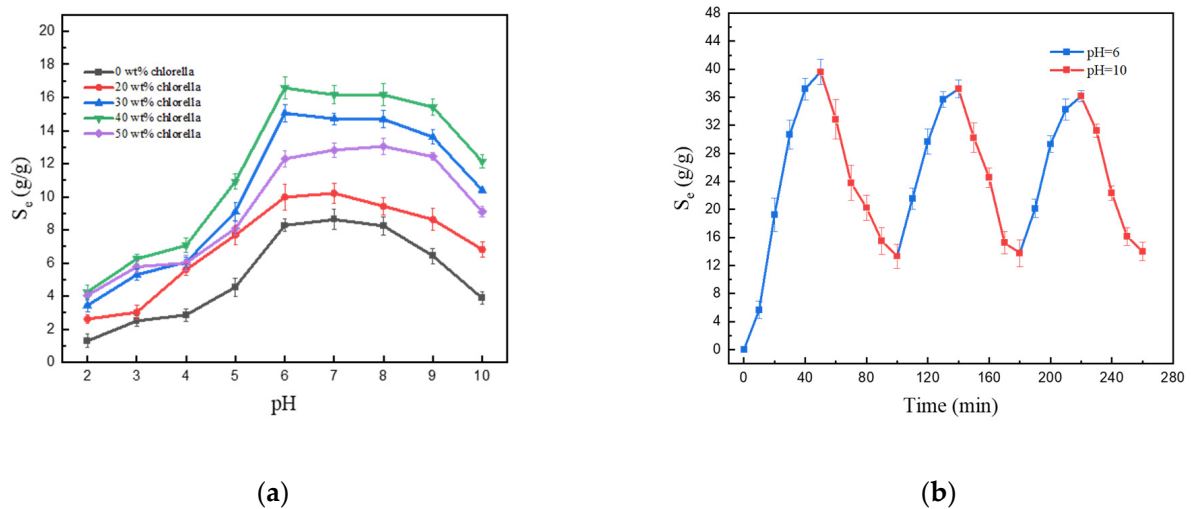
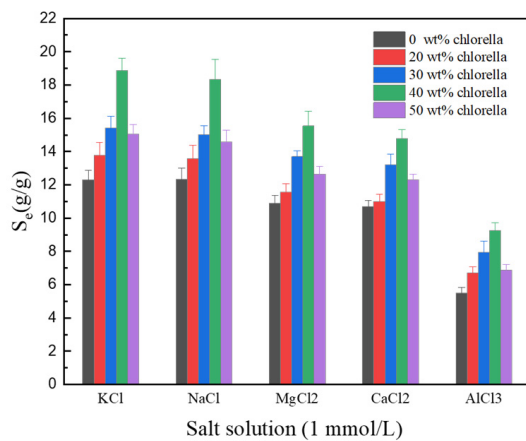


**Figure 5.** (a) Swelling ratio of chitosan–chlorella hydrogel beads in buffer solutions with various pH; (b) Reversible swelling of chitosan–chlorella hydrogel beads with 40 wt% *Chlorella* content at pH 6 and pH 10.

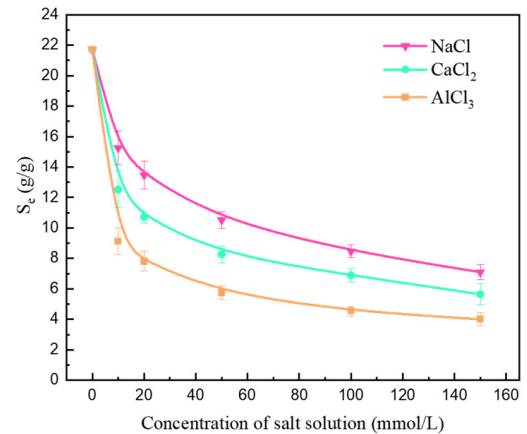
In order to study the swelling reversibility of beads, the chitosan–chlorella hydrogel beads with optimal water absorption were selected to be alternately immersed in solutions at two pH values of 6 and 10 to study pH-dependent swelling reversibility. It can be seen from the Figure 5b that the swelling of the chitosan–chlorella hydrogel beads is pH-dependence and reversible with a relatively quick speed. When the beads were in a buffer solution with pH 6, they swelled because of electrostatic repulsion due to amino protonation and shrinks at pH 10 due to deprotonation leads to the disappearance of electrostatic repulsion. The results showed the swelling–deswelling behavior of chitosan–chlorella hydrogel beads exhibited good pH-dependent reversibility and could be repeated many times.

### 3.3.2. Effect of Various Salt Solutions on Water Absorbency

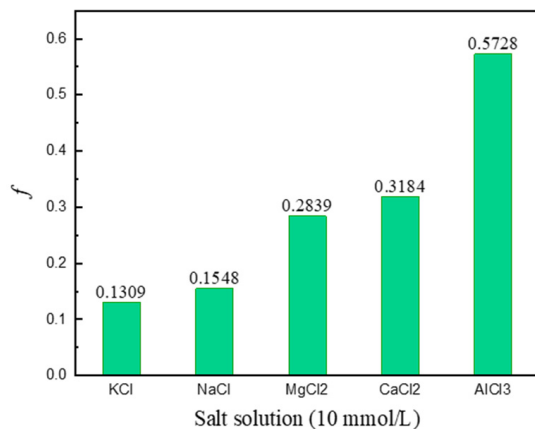
The swelling degree of chitosan–chlorella hydrogel beads influenced by different cations can be summarized from Figure 6a. The water absorption of the beads in salt solution was significantly lower than that in distilled water. In the swelling of ionic hydrogels, which is a common phenomenon, it is usually due to anion–anion electrostatic repulsion caused by the charge screening effect of cations and osmotic pressure difference between the inside and outside of the hydrogel network [37]. As can be seen from Figure 6a, the swelling ratio of hydrogel beads in different salt solutions were ranked from highest to lowest as  $\text{KCl} > \text{NaCl} > \text{MgCl}_2 > \text{CaCl}_2 > \text{AlCl}_3$ . This may be due to the complexation of polyvalent metal cations and hydroxyl groups on chitosan and the influence of ionic strength.



(a)



(b)



(c)

**Figure 6.** (a) Water absorbency of chitosan–chlorella hydrogel beads in salt solutions (1 mmol/L); (b) Influence of salt concentrations on the equilibrium swelling degree of chitosan–chlorella hydrogel beads with 40 wt% *Chlorella* content; (c) Salt sensitivity factors of chitosan–chlorella hydrogel beads with 40 wt% *Chlorella* content at a concentration of 10 mmol·L<sup>−1</sup>.

The swelling of chitosan–chlorella hydrogel beads in different concentrations of NaCl, CaCl<sub>2</sub>, and AlCl<sub>3</sub> salt solutions was studied as shown in Figure 6b. Two conclusions were obtained from Figure 6b: First, the swelling ratio of the hydrogel beads decreased with increasing concentrations of saline solution. This phenomenon was attributed to the fact that when the concentration of the salt solution increased, the concentration difference of the ions between the internal and external saline solution of the hydrogel network became smaller and the osmotic pressure difference decreased. The high salt concentration resulted in high external osmotic pressures, and in order to counteract the increase in external osmotic pressure, water molecules diffused from the inside to the outside of the hydrogel network, ultimately leading to a decrease in water uptake at equilibrium [38]. Second, the water absorption ability of hydrogels in various salt solution at the same concentration from high to low was Na<sup>+</sup> > Ca<sub>2</sub><sup>+</sup> > Al<sub>3</sub><sup>+</sup>. The data in Table 1 showed that the ionic strength is ordered as Al<sub>3</sub><sup>+</sup> > Ca<sub>2</sub><sup>+</sup> > Na<sup>+</sup> under the same concentration of the salt solution. That is, the swelling degree of the hydrogel beads decreased when the ionic strength of the external

salt solution increased. The influence of ionic strength on the swelling of hydrogel can be calculated through Flory's equation [39]:

$$S^{5/3} \approx \frac{(i/2V_u I^{1/2})^2 + (1/2 - X_i)/V_1}{V_e/V_0} \quad (5)$$

where  $S$  is the degree of swelling,  $i/V_u$  is the electric charge density of hydrogel,  $I$  is the ionic strength of external solution,  $(1/2 - X_i)/V_1$  is affinity of the hydrogel and the swelling medium, and  $V_e/V_0$  is the cross-link density.

**Table 1.** Effect of salt solutions on swelling ratio.

Solution (10 mmol/L)	Ionic Strength <sup>1</sup> (mol ion/dm <sup>3</sup> )	$S_e$ (g/g)
NaCl	0.01	15.25
CaCl <sub>2</sub>	0.03	12.52
AlCl <sub>3</sub>	0.06	9.12

<sup>1</sup>  $I = \frac{1}{2} \sum (C_i Z_i^2)$ , where  $I$  is the ionic strength of the saline solution,  $C_i$  is each ionic concentration of the saline solution, and  $Z_i$  is the charge number of the corresponding ion.

In order to contrast the sensitivity difference of chitosan–chlorella hydrogel beads to different swelling media, a dimensionless salt sensitivity factor  $f$  for 10 mmol·L<sup>−1</sup> salt solution was designed and could be calculated by the following formula [40]:

$$f = 1 - \frac{S_g}{S_d} \quad (6)$$

where  $S_g$  and  $S_d$  are the water absorption in given fluid and in distilled water, respectively. Figure 6c shows the dimensionless salt sensitive factor of chitosan–chlorella hydrogel beads in various salt solutions with the same concentration of 10 mmol/L. The higher the  $f$  value becomes, the greater the salt sensitivity is observed, and the lower the swelling degree in the corresponding fluid. As shown in Figure 6c, the  $f$  value is related to the charge number of the metal cation. More specifically, the salt sensitivities of different multivalent saline solutions are in the order of monovalent > divalent > trivalent cations. The AlCl<sub>3</sub> solution exhibit the strongest salt sensitivity, and here, the anti-swelling effect of ionic crosslinking plays a more critical role compared to the charge shielding effect.

### 3.3.3. Effect of Various Temperature on Water Absorbency

Figure 7 demonstrates the effect of the temperature on swelling of chitosan–chlorella hydrogel beads. It is obvious that the swelling degree decreased significantly with the increasing temperature. When the temperature was low (20~40 °C), the swelling rate of the chitosan–chlorella hydrogel beads with high content of *Chlorella* was significantly higher than that without *Chlorella*. When the temperature was high (50, 60 °C), the swelling rate of hydrogel beads decreased significantly due to the breakage of hydrogen bonds. At lower temperature, the presence of *Chlorella* makes it easier for water molecules to diffuse into the hydrogel. Therefore, the swelling ratio of hydrogel beads with high *Chlorella* content is stronger. When the temperature increased to 60 °C, *Chlorella* lost its bioactivity at high temperature, resulting in the swelling ratio of the hydrogel beads with high *Chlorella* content decreasing to the same level as that with low *Chlorella* content. The presence of *Chlorella* cells in the hydrogel network enhanced the water retention property to a certain extent, which indicated that *Chlorella* was feasible as a filling biomaterial.

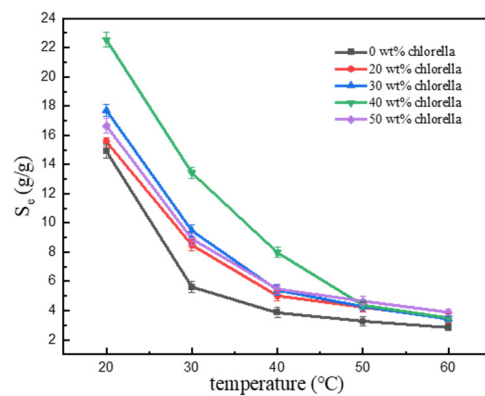


Figure 7. Swelling ratio of chitosan–chlorella hydrogel beads in distilled water at various temperatures.

### 3.4. Swelling Kinetics in Distilled Water

The time-dependent swelling process of the chitosan–chlorella hydrogel beads with various *Chlorella* contents in distilled water was given in Figure 8a. The swelling degree of samples increased rapidly at first, and then the rate of increase gradually reduced. The final state of swelling equilibrium was achieved after approximately 50 min. During the swelling process, water needed to continuously overcome the osmotic pressure inside the hydrogel. The higher the difference of osmotic pressure, the faster the water diffused into the hydrogel beads. As the hydrogel beads swelled by water absorption, the osmotic pressure difference between the inside and outside of the beads continuously decreased, and the swelling rate gradually decreased and finally reached equilibrium.

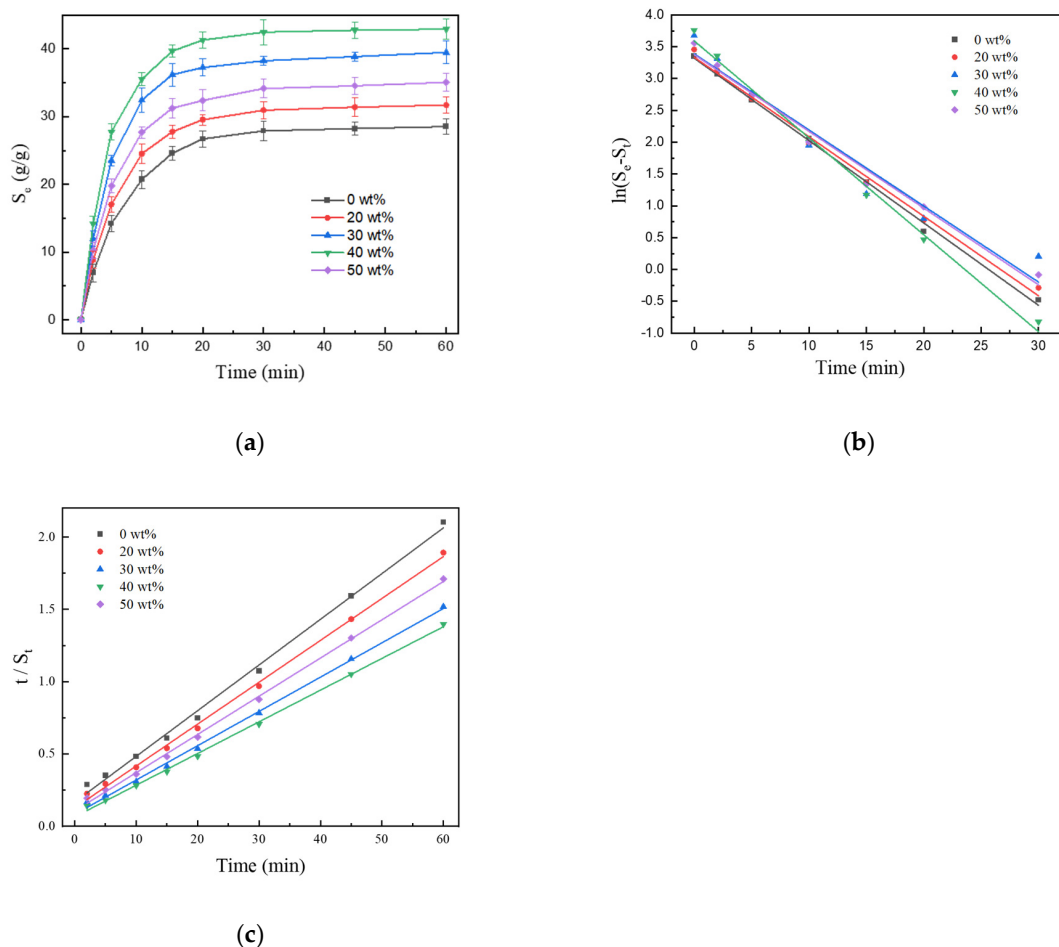


Figure 8. (a) Swelling process of chitosan–chlorella hydrogel beads in distilled water; (b) pseudo-first-order kinetics model; and (c) pseudo-second-order kinetics model.

To investigate the swelling kinetics mechanism of hydrogels in distilled water, the pseudo-first-order and pseudo-second-order models were employed to fit the experimental data. The pseudo-first-order swelling kinetic model was based on the assumption that adsorption is controlled by diffusion processes, and the adsorption ratio was dependent on the number of remaining adsorption sites. This swelling kinetic model could be given by the following equation [41]:

$$\ln(S_e - S_t) = \ln S_e - \frac{K_1 t}{2.303} \quad (7)$$

While the pseudo-second-order kinetics model could be expressed as the following formula:

$$\frac{t}{S_t} = \frac{1}{K_2 S_e^2} + \frac{t}{S_e} \quad (8)$$

where  $S_e$  (g/g) is the equilibrium swelling ratio,  $S_t$  (g/g) is the swelling ratio at contact time  $t$  (min), and  $K_1$  and  $K_2$  are the pseudo-first-order rate constant ( $\text{min}^{-1}$ ) and the pseudo-second-order rate constant ( $\text{g} \cdot \text{mg}^{-1} \cdot \text{min}^{-1}$ ), respectively.

As a result, the fitted curves of the swelling process obtained by the pseudo-first-order and pseudo-second-order kinetic models were presented in Figure 8b,c. The values of  $K_1$ ,  $K_2$ ,  $S_e$ , and the correlation coefficients ( $R^2$ ) are given in Table 2. The  $R^2$  value of the pseudo-second-order kinetics model was closer to one. Furthermore, the  $S_e$  value calculated by the pseudo-second-order kinetic model were closer to experimental data than those obtained by the pseudo-first-order model. It means that the pseudo-second-order model fits the data better than the pseudo-first-order model. Thus, this swelling process better fits the pseudo-second-order kinetic model.

**Table 2.** Kinetic parameters in the swelling process of chitosan–chlorella hydrogel beads.

Sample (Chlorella Contents)	$S_e$ (g/g)	Pseudo-First-Order			Pseudo-Second-Order		
		$K_1$	$R^2$	$S_e$ (g/g)	$K_2$	$R^2$	$S_e$ (g/g)
0 wt%	28.53	0.2981	0.9978	27.67	0.00595	0.9963	31.64
20 wt%	31.71	0.2877	0.9946	28.06	0.00658	0.9980	34.52
30 wt%	39.49	0.2753	0.9486	29.59	0.00678	0.9981	42.16
40 wt%	42.92	0.3507	0.9938	36.28	0.00074	0.9984	45.62
50 wt%	35.08	0.2775	0.9857	29.21	0.00656	0.9984	37.82

### 3.5. Application of Chitosan–Chlorella Hydrogel Beads for Loading and Controlled Release of Humic Acid

Humic substances are widely found in soils and water bodies in nature [42]. Humic acids have the effect of improving soil physicochemical properties and increasing grain yield [43]. In addition, humic acids can prevent nutrient degradation and loss, thereby reducing the use of inorganic fertilizers and improving fertilization efficiency. Actually, humic acids express as mixture of multiple dibasic acids, and their compositions are relatively complex: They can be divided into humic acids (HA), fluvic acids (FA), and humins based their solubility in acid–base solution. HA is soluble in base but insoluble in acid, FA is soluble in both base and acid, and humins are soluble in dilute base but insoluble in acid and water [44]. A simple and controllable use method has a significant role in agricultural applications of humic acids. Therefore, we chose humic acid as a model fertilizer to study the controlled release ability of hydrogel beads. For this purpose, the pH- and temperature-responsive chitosan–chlorella hydrogel beads with 40 wt% *Chlorella* content were selected as the matrix material, and the loading and slow-release efficiency for humic acid were investigated.

### 3.5.1. Loading Efficiency of Hydrogel Beads for Humic Acid

Figure 9a shows the influence of pH on the loading efficiency of humic acid in hydrogel beads with 40 wt% *Chlorella* content. The loading of humic acid gradually reached equilibrium with the swelling process of the beads. When the solution pH was 4, the loading efficiency of humic acid was higher, the maximum loading rate was 83.6%, and it decreased obviously as the pH increased from 4 to 10. During the loading process, the interaction between the chitosan–chlorella hydrogel beads and humic acid was mainly the complexation of protonated amino groups on chitosan with carboxyl or phenolic groups in humic acid [45]. In lower pH solution, more amino groups on chitosan were protonated, while protonated amino groups can combine with  $-\text{COOH}$  in humic acid, thus greater adsorption was obtained. Moreover, from the point of view of electrostatic action, the protonated amino groups on chitosan express electrostatic attraction to humic acid at  $\text{pH} < 6$ . However, when the pH was 2, the chitosan–chlorella hydrogel beads were corroded by acidic solution, which resulted in the destruction of the crosslinked network structure and lower loading efficiency of humic acid.

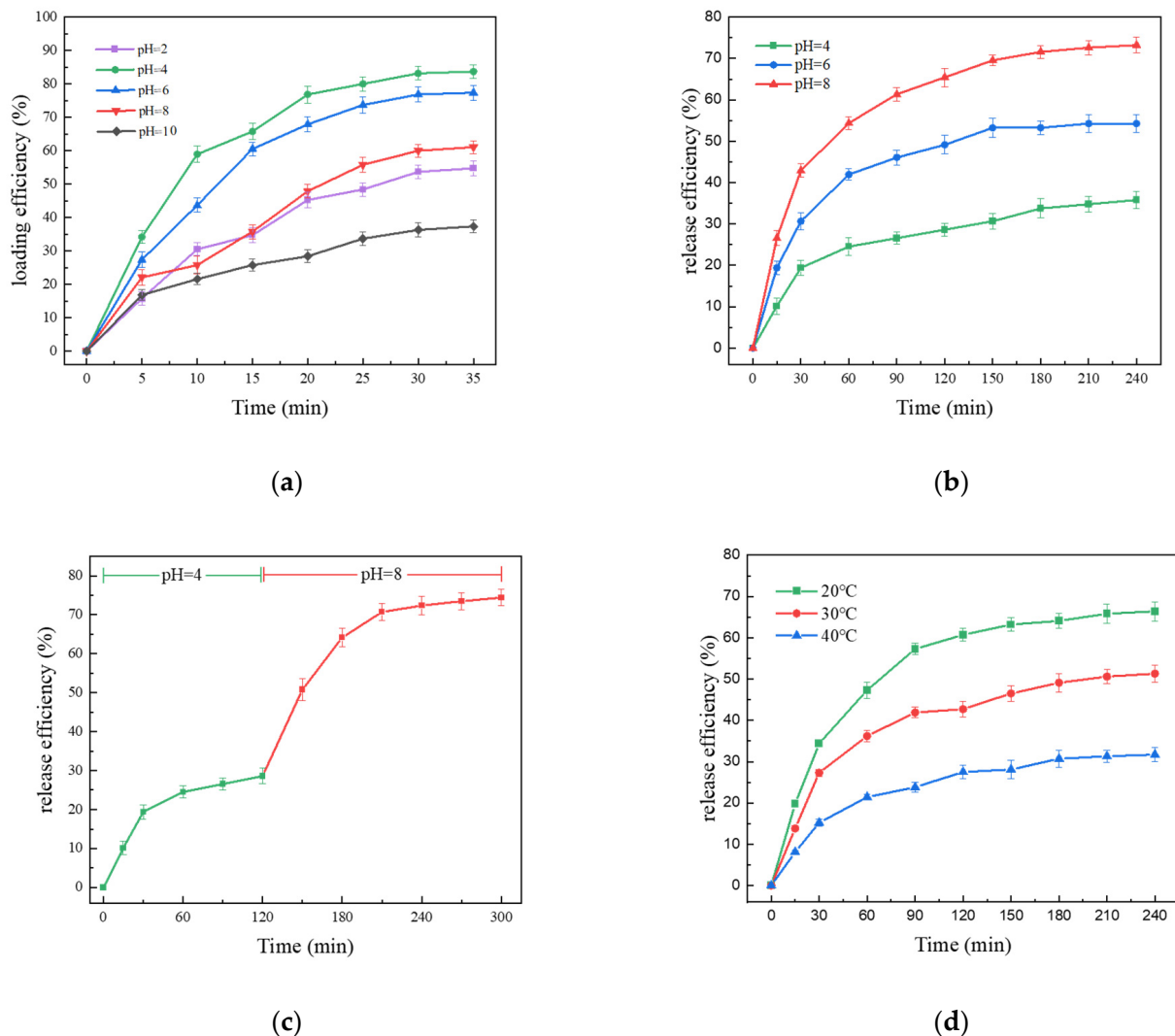


**Figure 9.** (a) the influence of pH to the efficiency for humic acid loading of chitosan–chlorella hydrogel beads with 40% *Chlorella* content; (b) release percentage of humic acid from chitosan–chlorella hydrogel beads under different pH; (c) Progressive controlled release of humic acid from chitosan–chlorella hydrogel beads at pH 4 and 8; (d) release percentage of humic acid from chitosan–chlorella hydrogel beads under different temperatures.

### 3.5.2. pH-Responsive Release Behavior of Hydrogel Beads

Figure 9b shows the release efficiency of the beads loaded with humic acid with various pH. The results indicated that the slow-release of humic acid was a pH-responsive process. The slow-release efficiency increased at high pH, and the release reached a balance of 35.8%, 54.2%, and 73.2% at pH 4, 6, and 8, respectively. With high pH of the in vitro solution, the humic acids were released as more protonated amino groups on chitosan were deprotonated. Meanwhile the slow-release is also limited by the hydrogen bonding effect between chitosan and humic acid. Specifically, hydrogen bonds between amino groups on chitosan and carboxyl or phenolic groups in humic acid prevented the humic acid from releasing. There was also a portion of humic acids trapped in the cross-linked network that could not be released, resulting in a slow-release efficiency below 100%.

Considering that the release process was a pH-dependent behavior, the pH-responsive controlled release of the loaded humic acid was investigated by changing the pH of external solution. The beads containing humic acid were first placed into distilled water at pH 4 for 120 min, and then the pH was changed to 8. The results of controlled release efficiency are shown in Figure 9c. The release rate was slower at pH 4, and the release efficiency reached 20% at 120 min. When pH was changed to 8, a dramatic step change in the release efficiency of humic acid release occurred, and more time was required to reach equilibrium, with the release efficiency eventually reaching approximately 80%. In summary, the pH-responsive controlled release of humic acid demonstrated that the chitosan–chlorella hydrogel beads could respond to the pH changes in the external solution, which indicated the potential of chitosan–chlorella hydrogel beads as carrier materials for controlled release.

### 3.5.3. Temperature-Responsive Release Behavior of Hydrogel Beads

In addition to pH-responsive capacity, the sensitivity of chitosan–chlorella hydrogel beads to temperature allows for temperature-responsive controlled release. Figure 9d shows the cumulative release of humic acid at various temperatures (20 °C, 30 °C, and 40 °C). The cumulative release percentage decreased with increasing temperature, and the fastest release rate was achieved at 20 °C with the final cumulative release percentage of 66.4%, which was higher than those at 20 °C and 30 °C under the same conditions. It may be attributed to the enhanced swelling properties, where hydrogel beads have better water absorption properties at lower temperatures and humic acids are easier to release into the medium from the expanded cross-linked network.

## 4. Conclusions

In summary, we successfully prepared eco-friendly chitosan–chlorella hydrogel beads with various *Chlorella* contents in a facile and economical method and explored the synthesis mechanism in detail. The introduction of *Chlorella* into chitosan matrix brought enhanced mechanical stability and better swelling properties to the chitosan–chlorella hydrogel beads. The enhanced mechanical stability allowed the hydrogel beads to retain more water when facing ultrasound or centrifugation. Chitosan–chlorella hydrogel beads were obviously responsive to the external factors such as the pH value, saline solution concentration and temperature, specifically in the form of differences in swelling degree. The resultant hydrogel beads with 40 wt% *Chlorella* content reached the maximum swelling degree of 42.92 g/g in distilled water, and swelling behavior was better fitted to the pseudo-second-order kinetic model. In addition, chitosan–chlorella hydrogel beads are stimulated responsive to pH and temperature during slow release and can better cope with the complex environment of practical agricultural controlled release fertilizer applications.

**Author Contributions:** Conceptualization, Y.L. and B.B.; methodology, H.L. and J.W.; software, H.L. and J.W.; validation, H.L., J.W., F.C. and Y.L.; formal analysis, B.B. and Y.L.; investigation, H.L. and J.W.; resources, B.B. and Y.L.; data curation, H.L.; writing—original draft preparation, H.L.; writing—review and editing, Y.L., B.B. and F.C.; visualization, H.L. and J.W.; supervision, Y.L. and B.B.; project administration, B.B.; funding acquisition, B.B. and Y.L. All authors have read and agreed to the published version of the manuscript.

**Funding:** This research was funded by the Natural Science Basic Research Program of Shaanxi, Program No. 2021SF-497 and No. 2022TD-04, and the Fundamental Research Funds for the Central Universities, CHD 300102290103, CHD 300102291403, and CHD 300102292903, and Shaanxi Water Conservancy Science and technology project, 2015slkj-02.

**Institutional Review Board Statement:** Not applicable.

**Informed Consent Statement:** Not applicable.

**Data Availability Statement:** Not applicable.

**Conflicts of Interest:** The authors declare no conflict of interest.

## References

1. Zhong, K.; Lin, Z.T.; Zheng, X.L.; Jiang, G.B.; Fang, Y.S.; Mao, X.Y.; Liao, Z.W. Starch derivative-based superabsorbent with integration of water-retaining and controlled-release fertilizers. *Carbohydr. Polym.* **2013**, *92*, 1367–1376. [[CrossRef](#)] [[PubMed](#)]
2. Castro, G.; Zotarelli, L.; Mattiello, E.M.; Tronto, J. Alginate beads containing layered double hydroxide intercalated with borate: A potential slow-release boron fertilizer for application in sandy soils. *New J. Chem.* **2020**, *44*, 16965–16976. [[CrossRef](#)]
3. Ramli, R.A. Slow release fertilizer hydrogels: A review. *Polym. Chem.* **2019**, *10*, 6073–6090. [[CrossRef](#)]
4. Lin, X.Y.; Guo, L.Z.; Shaghaleh, H.; Hamoud, Y.A.; Xu, X.; Liu, H. A TEMPO-oxidized cellulose nanofibers/MOFs hydrogel with temperature and pH responsiveness for fertilizers slow-release. *Int. J. Biol. Macromol.* **2021**, *191*, 483–491. [[CrossRef](#)]
5. Zhao, Y.X.; Fan, Z.; Chen, Y.R.; Huang, X.X.; Zhai, S.; Sun, S.C.; Tian, X.F. A Bio-Based Hydrogel Derived from Moldy Steamed Bread as Urea-Formaldehyde Loading for Slow-Release and Water-Retention Fertilizers. *ACS Omega* **2021**, *6*, 33462–33469. [[CrossRef](#)]
6. Singh, A.; Kar, A.K.; Singh, D.; Verma, R.; Shraogi, N.; Zehra, A.; Gautam, K.; Anbumani, S.; Ghosh, D.; Patnaik, S. pH-responsive eco-friendly chitosan modified cenosphere/alginate composite hydrogel beads as carrier for controlled release of Imidacloprid towards sustainable pest control. *Chem. Eng. J.* **2022**, *427*, 131215. [[CrossRef](#)]
7. Bakshi, P.S.; Selvakumar, D.; Kadirvelu, K.; Kumar, N.S. Chitosan as an environment friendly biomaterial—A review on recent modifications and applications. *Int. J. Biol. Macromol.* **2020**, *150*, 1072–1083. [[CrossRef](#)]
8. Choi, C.; Nam, J.-P.; Nah, J.-W. Application of chitosan and chitosan derivatives as biomaterials. *J. Ind. Eng. Chem.* **2016**, *33*, 1–10. [[CrossRef](#)]
9. Khoushab, F.; Yamabhai, M. Chitin Research Revisited. *Mar. Drugs* **2010**, *8*, 1988–2012. [[CrossRef](#)]
10. Aranaz, I.; Harris, R.; Heras, A. Chitosan Amphiphilic Derivatives. Chemistry and Applications. *Curr. Org. Chem.* **2010**, *14*, 308–330. [[CrossRef](#)]
11. Genta, I.; Perugini, P.; Pavanetto, F. Different molecular weight chitosan microspheres: Influence on drug loading and drug release. *Drug Dev. Ind. Pharm.* **1998**, *24*, 779–784. [[CrossRef](#)] [[PubMed](#)]
12. Wu, T.; Yu, S.; Lin, D.; Wu, Z.; Xu, J.; Zhang, J.; Ding, Z.; Miao, Y.; Liu, T.; Chen, T.; et al. Preparation, Characterization, and Release Behavior of Doxorubicin hydrochloride from Dual Cross-Linked Chitosan/Alginate Hydrogel Beads. *ACS Appl. Bio Mater.* **2020**, *3*, 3057–3065. [[CrossRef](#)] [[PubMed](#)]
13. Yang, I.H.; Lin, I.E.; Chen, T.C.; Chen, Z.Y.; Lin, F.H. Synthesis, Characterization, and Evaluation of BDDE Crosslinked Chitosan-TGA Hydrogel Encapsulated with Genistein for Vaginal Atrophy. *Carbohydr. Polym.* **2021**, *260*, 117832. [[CrossRef](#)] [[PubMed](#)]
14. Shawky, H.A.; El-Aassar, A.H.M.; Abo-Zeid, D.E. Chitosan/carbon nanotube composite beads: Preparation, characterization, and cost evaluation for mercury removal from wastewater of some industrial cities in Egypt. *J. Appl. Polym. Sci.* **2011**, *125*, E93–E101. [[CrossRef](#)]
15. Monvisade, P.; Siriphannon, P. Chitosan intercalated montmorillonite: Preparation, characterization and cationic dye adsorption. *Appl. Clay Sci.* **2009**, *42*, 427–431. [[CrossRef](#)]
16. Mokhothu, T.H.; John, M.J.; John, M.J. Bio-Based Fillers for Environmentally Friendly Composites. In *Handbook of Composites from Renewable Materials*; Vijay, K.T., Manju, K.T., Michael, R.K., Eds.; Scrivener Publishing LLC: Beverly, MA, USA, 2017; pp. 243–270. [[CrossRef](#)]
17. Murawski, A.; Diaz, R.; Inglesby, S.; Delabar, K.; Quirino, R.L. Synthesis of Bio-based Polymer Composites: Fabrication, Fillers, Properties, and Challenges. In *Polymer Nanocomposites in Biomedical Engineering*; Sadasivuni, K.K., Ponnamma, D., Rajan, M., Ahmed, B., Al-Maadeed, M.A.S.A., Eds.; Springer International Publishing: Cham, Switzerland, 2019; pp. 29–55. [[CrossRef](#)]
18. Yuan, Q.; Li, H.; Wei, Z.; Lv, K.; Gao, C.; Liu, Y.; Zhao, L. Isolation, structures and biological activities of polysaccharides from *Chlorella*: A review. *Int. J. Biol. Macromol.* **2020**, *163*, 2199–2209. [[CrossRef](#)]
19. Chen, Y.; Liu, X.; Wu, L.; Tong, A.; Zhao, L.; Liu, B.; Zhao, C. Physicochemical characterization of polysaccharides from *Chlorella pyrenoidosa* and its anti-ageing effects in *Drosophila melanogaster*. *Carbohydr. Polym.* **2018**, *185*, 120–126. [[CrossRef](#)]
20. Safi, C.; Zebib, B.; Merah, O.; Pontalier, P.-Y.; Vaca-Garcia, C. Morphology, composition, production, processing and applications of *Chlorella vulgaris*: A review. *Renew. Sustain. Energ. Rev.* **2014**, *35*, 265–278. [[CrossRef](#)]
21. Takeda, H. Sugar Composition of the Cell Wall and the Taxonomy of *Chlorella* (Chlorophyceae). *J. Phycol.* **1991**, *27*, 224–232. [[CrossRef](#)]

22. Gunerken, E.; D'Hondt, E.; Eppink, M.H.; Garcia-Gonzalez, L.; Elst, K.; Wijffels, R.H. Cell disruption for microalgae biorefineries. *Biotechnol. Adv.* **2015**, *33*, 243–260. [[CrossRef](#)]
23. Wang, L.; Addy, M.; Lu, Q.; Cobb, K.; Chen, P.; Chen, X.; Liu, Y.; Wang, H.; Ruan, R. Cultivation of *Chlorella vulgaris* in sludge extracts: Nutrient removal and algal utilization. *Bioresour. Technol.* **2019**, *280*, 505–510. [[CrossRef](#)] [[PubMed](#)]
24. Mhatre, A.M.; Raja, A.S.M.; Saxena, S.; Patil, P.G. Environmentally Benign and Sustainable Green Composites: Current Developments and Challenges. In *Green Composites: Sustainable Raw Materials*; Muthu, S.S., Ed.; Springer: Singapore, 2019; pp. 53–90. [[CrossRef](#)]
25. Yang, S.; Hu, J.; Chen, C.; Shao, D.; Wang, X. Mutual Effects of Pb(II) and Humic Acid Adsorption on Multiwalled Carbon Nanotubes/Polyacrylamide Composites from Aqueous Solutions. *Environ. Sci. Technol.* **2011**, *45*, 3621–3627. [[CrossRef](#)] [[PubMed](#)]
26. Xie, C.-X.; Tian, T.-C.; Yu, S.-T.; Li, L. pH-sensitive hydrogel based on carboxymethyl chitosan/sodium alginate and its application for drug delivery. *J. Appl. Polym. Sci.* **2019**, *136*, 46911. [[CrossRef](#)]
27. Wu, X.; Li, H. Incorporation of Bioglass Improved the Mechanical Stability and Bioactivity of Alginate/Carboxymethyl Chitosan Hydrogel Wound Dressing. *ACS Appl. Bio Mater.* **2021**, *4*, 1677–1692. [[CrossRef](#)]
28. Li, N.; Bai, R. Copper adsorption on chitosan–cellulose hydrogel beads: Behaviors and mechanisms. *Sep. Purif. Technol.* **2005**, *42*, 237–247. [[CrossRef](#)]
29. Pourjavadi, A.; Aghajani, V.; Ghasemzadeh, H. Synthesis, characterization and swelling behavior of chitosan-sucrose as a novel full-polysaccharide superabsorbent hydrogel. *J. Appl. Polym. Sci.* **2010**, *109*, 2648–2655. [[CrossRef](#)]
30. Phukan, M.M.; Chutia, R.S.; Konwar, B.K.; Katak, R. Microalgae *Chlorella* as a potential bio-energy feedstock. *Appl. Energ.* **2011**, *88*, 3307–3312. [[CrossRef](#)]
31. Jafari, Y.; Sabahi, H.; Rahaie, M. Stability and loading properties of curcumin encapsulated in *Chlorella vulgaris*. *Food Chem.* **2016**, *211*, 700–706. [[CrossRef](#)]
32. Patra, T.; Pal, A.; Dey, J. A smart supramolecular hydrogel of N(alpha)-(4-n-alkyloxybenzoyl)-L-histidine exhibiting pH-modulated properties. *Langmuir* **2010**, *26*, 7761–7767. [[CrossRef](#)]
33. Cong, H.P.; Wang, P.; Yu, S.H. Highly Elastic and Superstretchable Graphene Oxide/Polyacrylamide Hydrogels. *Small* **2014**, *10*, 448–453. [[CrossRef](#)]
34. Atassi, Y.; Said, M.; Tally, M.; Kouba, L. Synthesis and characterization of chitosan-g-poly(AMPS-co-AA-co-AM)/ground basalt composite hydrogel: Antibacterial activity. *Polym. Bull.* **2019**, *77*, 5281–5302. [[CrossRef](#)]
35. Shi, X.; Wang, W.; Wang, A. Synthesis and enhanced swelling properties of a guar gum-based superabsorbent composite by the simultaneous introduction of styrene and attapulgit. *J. Polym. Res.* **2011**, *18*, 1705–1713. [[CrossRef](#)]
36. Hayati, M.; Rezanejade Bardajee, G.; Ramezani, M.; Hosseini, S.S.; Mizani, F. Temperature/pH/magnetic triple-sensitive nanogel–hydrogel nanocomposite for release of anticancer drug. *Polym. Int.* **2019**, *69*, 156–164. [[CrossRef](#)]
37. Akar, E.; Altinisik, A.; Seki, Y. Preparation of pH- and ionic-strength responsive biodegradable fumaric acid crosslinked carboxymethyl cellulose. *Carbohydr. Polym.* **2012**, *90*, 1634–1641. [[CrossRef](#)]
38. Li, Q.; Ma, Z.; Yue, Q.; Gao, B.; Li, W.; Xu, X. Synthesis, characterization and swelling behavior of superabsorbent wheat straw graft copolymers. *Bioresour. Technol.* **2012**, *118*, 204–209. [[CrossRef](#)]
39. Bao, Y.; Ma, J.; Li, N. Synthesis and swelling behaviors of sodium carboxymethyl cellulose-g-poly(AA-co-AM-co-AMPS)/MMT superabsorbent hydrogel. *Carbohydr. Polym.* **2011**, *84*, 76–82. [[CrossRef](#)]
40. Pourjavadi, A.; Barzegar, S.; Mahdavinia, G.R. MBA-crosslinked Na-Alg/CMC as a smart full-polysaccharide superabsorbent hydrogels. *Carbohydr. Polym.* **2006**, *66*, 386–395. [[CrossRef](#)]
41. Liu, D.; Li, Z.; Li, W.; Zhong, Z.; Xu, J.; Ren, J.; Ma, Z. Adsorption Behavior of Heavy Metal Ions from Aqueous Solution by Soy Protein Hollow Microspheres. *Ind. Eng. Chem. Res.* **2013**, *52*, 11036–11044. [[CrossRef](#)]
42. Ndzelu, B.S.; Dou, S.; Zhang, X.W. Changes in soil humus composition and humic acid structural characteristics under different corn straw returning modes. *Soil Res.* **2020**, *58*, 452–460. [[CrossRef](#)]
43. Jing, J.; Zhang, S.; Yuan, L.; Li, Y.; Lin, Z.; Xiong, Q.; Zhao, B. Combining humic acid with phosphate fertilizer affects humic acid structure and its stimulating efficacy on the growth and nutrient uptake of maize seedlings. *Sci. Rep.* **2020**, *10*, 17502. [[CrossRef](#)]
44. Feizollahi, E.; Mirmahdi, R.S.; Zoghi, A.; Zijlstra, R.T.; Vasanthan, T. Review of the beneficial and anti-nutritional qualities of phytic acid, and procedures for removing it from food products. *Food Res. Int.* **2021**, *143*, 110284. [[CrossRef](#)] [[PubMed](#)]
45. Yan, W.L.; Bai, R. Adsorption of lead and humic acid on chitosan hydrogel beads. *Water Res.* **2005**, *39*, 688–698. [[CrossRef](#)] [[PubMed](#)]